A comparison study on the electronic structures, lattice dynamics and thermoelectric properties of bulk silicon and silicon nanotubes*

Lu Peng-Xian(路朋献)†, Qu Ling-Bo(屈凌波), and Cheng Qiao-Huan(程巧换)

College of Materials Science and Engineering, Henan University of Technology, Zhengzhou 450001, *China*
College of Chemistry and Molecular Engineering, Zhengzhou University, Zhengzhou 450001, *China*

(Received 12 April 2013; revised manuscript received 30 May 2013)

In order to investigate the mechanism of the electron and phonon transport in a silicon nanotube (SiNT), the electronic structures, the lattice dynamics, and the thermoelectric properties of bulk silicon (bulk Si) and a SiNT have been calculated in this work using density functional theory and Boltzmann transport theory. Our results suggest that the thermal conductivity of a SiNT is reduced by a factor of 1, while its electrical conductivity is improved significantly, although the Seebeck coefficient is increased slightly as compared to those of the bulk Si. As a consequence, the figure of merit (ZT) of a SiNT at 1200 K is enhanced by 12 times from 0.08 for bulk Si to 1.10. The large enhancement in electrical conductivity originates from the largely increased density of states at the Fermi energy level and the obviously narrowed band gap. The significant reduction in thermal conductivity is ascribed to the remarkably suppressed phonon thermal conductivity caused by a weakened covalent bonding, a decreased phonon density of states, a reduced phonon vibration frequency, as well as a shortened mean free path of phonons. The other factors influencing the thermoelectric properties have also been studied from the perspective of electronic structures and lattice dynamics.

Keywords: electronic structure, lattice dynamics, thermoelectric properties, silicon nanotube

PACS: 71.15.Mb, 72.15.Jf, 63.20.dk **DOI:** 10.1088/1674-1056/22/11/117101

1. Introduction

SiGe polycrystalline alloys, which can be used as thermoelectric generators in deep-space missions and small unattended terrestrial systems, have been proven to be highly reliable and long-lived power sources. Their coefficient is evaluated by a dimensionless figure of merit (ZT). A thermoelectric material with excellent performance needs a high electrical conductivity, a large Seebeck coefficient, and meanwhile a low thermal conductivity. Hence, the development of the ZT value for SiGe alloys is the key to improving the existing technology and expand it into larger-scale applications. In practice, they should have a peak ZT value as high as 1.0 at a temperature close to 1275 K. However, the optimal ZT value for SiGe alloys across the operating temperature range is only about 0.55, which induces a low conversion efficiency below 8%. To achieve a higher ZT value for SiGe alloys, nanostructuring has been considered as the most effective approach. Firstly, the electrical conductivity of a nanomaterial can be enhanced by increasing the density of states near the Fermi energy level. Secondly, the Seebeck coefficient can be optimized by improving the effective mass of carriers. Thirdly, the thermal conductivity can be reduced by introducing more interfaces into the material.[1,2] Recently, much attention has been paid to SiGe nanowires for their large reduction in phonon thermal conductivity.[3] The maximum ZT value for n-type $Si_{0.5}Ge_{0.5}$ nanowires could be increased by a factor of 4.3 theoretically as compared to pure Si nanowires.[4] However, a shortcoming for SiGe nanowires should not be ignored. The introduction of expensive and rare Ge into SiGe nanowires is very disadvantageous to their larger-scale applications.

Therefore, it is of significance to replace SiGe alloys or nanowires with abundant and low-cost silicon semiconductors. However, the ZT value of SiB is only 0.001 at room temperature due to its huge thermal conductivity. Very recently, it has been demonstrated that Si nanowires have a Seebeck coefficient and an electrical conductivity which are the same as those of the doped bulk Si, but exhibit a 100-fold reduction in thermal conductivity, yielding a ZT value of 0.6 at room temperature. Such large enhancement in the ZT value of Si nanowires arises from the significantly reduced phonon thermal conductivity, which approaches the limit of amorphous Si bulk.[5,6] Meanwhile, theoretical calculations have been conducted extensively to investigate the mechanism of the electron and phonon transport in Si nanowires. The ZT value of Si nanowires is expected to be increased by as much as 20 times as compared to that of bulk Si for its large reduction in phonon thermal conductivity.[7] The cross section shape will play an important role in the thermoelectric properties for Si nanowires since their extremely small size is accompanied by a strong quantum confinement effect. The ZT value of Si nanowires can be enhanced to 1.5 and 0.85 for n-doped and p-doped triangular Si nanowires.[8,9] Hence, it should be undoubted that the large enhancement in the ZT value of Si nanowires is attributed to the significant reduction in phonon

*Project supported by the Science Foundation of Henan University of Technology, China (Grant Nos. 2011BS056 and 11JCYJ12) and the Post-Doctor Science Research Fund of China (Grant No. 110832).

†Corresponding author. E-mail: pengxian_lu@haut.edu.cn

© 2013 Chinese Physical Society and IOP Publishing Ltd

thermal conductivity.

A larger ZT value for nanotubes should also be achieved due to their much lower thermal conductivity. A high Seebeck coefficient and a reasonable electrical conductivity can be realized in InSe nanotubes.[10] The thermoelectric properties of carbon nanotubes are associated with the diameter and the chirality, and thus can be optimized by surface design, formation of bundles, as well as tube length.[11,12] The effects of thickness, diameter, growth direction, and carrier concentration of Bi nanotubes on the ZT value have also been investigated.[13] It has been demonstrated theoretically that only a 1% reduction in cross section area of nanotubes can result in a 35% reduction in thermal conductivity. Moreover, the thermal conductivity of SiNTs is only about 33% of that of Si nanowires at room temperature due to their enhanced surface-to-volume ratio.[14] As a result, SiNTs should have great potential as a promising candidate to replace the expensive SiGe alloys or nanowires.

Unfortunately, very little work on SiNTs has been done and the mechanism of the electron and phonon transport in SiNTs is still undetermined.[15] Therefore, our work's aim is to provide a complete understanding of the mechanism of the electron and phonon transport in SiNTs by comparing the electronic structures, the lattice dynamics, and the thermoelectric properties of bulk Si and SiNTs.

2. Calculation methods

Bulk Si has a face-centered cubic symmetry (FD3-MS, Group No. 227) with a lattice constant of 0.543 nm, in which Si atoms occupy (0.0, 0.0, 0.0) site.[16] A 6×6 armchair chirality and a bonding length of 0.245 nm were taken to construct a single-wall SiNT with a diameter of 14.04 Å. Calculations were performed using the Cambridge Serial Total Energy Package (CASTEP), a first-principle pseudopotential method based on the density-functional theory (DFT).[17,18] The pseudopotential we used was the norm-conserving pseudopotential. As for the approximation of the exchange correlation term of the DFT, the Perdew's generalized gradient approximation (GGA) was adopted with Perdew–Burke–Ernzerhof parameters.[19] The cutoff energy of atomic wave functions was set at 390 eV. Sampling of the irreducible wedge of the Brillouin zone was performed with a regular Monkhorst-Pack grid of special k-points, which was 30 × 30 × 30 and 6 × 6 × 1 for bulk Si and the SiNT, respectively. The high-symmetry points in the Brillouin zone were selected as X (0.500, 0.000, 0.000), R (0.500, 0.500, 0.500), A (0.000, 0.000, 0.500), H (−0.333, 0.667, 0.500), K (−0.333, 0.667, 0.000), M (0.000, 0.500, 0.000), and L (0.000, 0.500, 0.500). A finite basis set correction and the Pulay scheme of density mixing were applied for the evaluation of energy. The effects of the electron spin on the electronic structure were also considered.[20,21] All atomic positions in our models have been relaxed according to the total energy and force using the BFGS scheme, based on the cell optimization criterion (RMs force of 0.01 eV/nm, displacement of 0.00002 nm). The calculation of total energy and electronic structure was followed by cell optimization with an SCF tolerance of 5.0×10^{-7} eV. The band structure and the phonon dispersion along several high-symmetry points in the Brillouin zone were calculated. The partial density of states (PDOS) for electrons and phonons was obtained by broadening the discrete energy levels using a smearing function of 0.05 eV full width at half maximum (FWHM) on a grid of k-points generated by the Monkhorst–Pack scheme.[22]

The temperature dependence of the heat capacity C and Debye temperature Θ_{D} are obtained by calculating the phonon dispersion. The mean free path λ of phonons is calculated by

$$\lambda = 10^{-8}\exp\left(\frac{\Theta_{\mathrm{D}}}{\eta T}\right), \tag{1}$$

where T is the absolute temperature, and η is a constant equal to 1.62, which depends on the scattering limitation of phonons.[23,24] The effective mass of carriers m^* can be obtained by differentiating the energy at the Fermi energy level twice with respect to the wave vector of the high-symmetry points in the Brillouin zone. The temperature dependence of the Fermi energy is calculated by

$$E_{\mathrm{F}} = E_{\mathrm{F}}^0\left[1-\frac{\pi^2}{12}\left(\frac{k_{\mathrm{B}}T}{E_{\mathrm{F}}^0}\right)^2\right], \tag{2}$$

where E_{F}^0 is the Fermi energy at 0 K, T is the absolute temperature, and k_{B} is the Boltzmann constant.[25] The Fermi–Dirac distribution function $(-\partial f/\partial E)$ is written as

$$\left(-\frac{\partial f}{\partial E}\right) = \frac{1}{k_{\mathrm{B}}T}\,\frac{1}{\left(\mathrm{e}^{(E-E_{\mathrm{F}})/k_{\mathrm{B}}T}+1\right)}\,\frac{1}{\left(\mathrm{e}^{-(E-E_{\mathrm{F}})/k_{\mathrm{B}}T}+1\right)}, \tag{3}$$

where E is the energy band. The group velocity of carriers $\upsilon_{\mathrm{e}}(E)$ is calculated by differentiating the energy with respect to the wave vector in the Brillouin zone.[26] Consequently, the electrical conductivity and the Seebeck coefficient are defined as[27–29]

$$\sigma = \frac{e^2}{3}\int \mathrm{d}E\left(-\frac{\partial f}{\partial E}\right)g(E)\tau(E)\upsilon^2(E), \tag{4}$$

$$\alpha = \frac{e}{3T\sigma}\int \mathrm{d}E\left(-\frac{\partial f}{\partial E}\right)g(E)\tau(E)\upsilon^2(E)(E-E_{\mathrm{F}}), \tag{5}$$

where e is the electron charge, $(-\partial f/\partial E)$ is the Fermi distribution function, $g(E)$ is the DOS, $\upsilon_{\mathrm{e}}(E)$ is the group velocity of electrons, E and E_{F} are the energy band and the Fermi energy, respectively. τ(E) is the relaxation time, which can be simplified as an energy-independent constant equal to 1.2×10^{-20} s using the experimental electrical conductivity.[30] The electron thermal conductivity κ_{e} is estimated using the Wiedemann–Franz law,[31] and the phonon thermal conductivity κ_{p} is given by[32]

$$\kappa_{\mathrm{p}} = \frac{1}{3}\rho\upsilon_{\mathrm{p}}C\lambda, \tag{6}$$

where ρ is the theoretical density equal to 1165 kg/m^3 and 930 kg/m^3 for bulk Si and the SiNT, respectively, C is the heat capacity, and υ_p represents the average velocity of phonons equal to 2658 m/s and 2270 m/s for bulk Si and the SiNT, respectively. The average velocity of phonons is calculated from the phonon dispersion by differentiating the frequency of phonons with respect to the wave factor of the high-symmetry points in the Brillouin zone. Therefore, the ZT is determined by

$$\mathrm{ZT} = \frac{\alpha^2\sigma}{\kappa_e+\kappa_p}T, \tag{7}$$

where α is the Seebeck coefficient, σ is the electrical conductivity, κ_e and κ_p are the thermal conductivity contributed from electrons and phonons, respectively, and T is the absolute temperature.

3. Results and discussion

3.1. Electronic structure

The partial density of states (PDOS) of bulk Si and the SiNT is presented in Figs. 1(a) and 1(b), respectively. A band gap of 0.63 eV is observed for bulk Si, indicating a typical semiconductor, but the SiNT exhibits a narrowed band gap of 0.31 eV. The electrical conductivity and Seebeck coefficient are influenced profoundly by the band gap. A small SiNT band gap is beneficial to a high electrical conductivity, but is disadvantageous to a large Seebeck coefficient.[33] It can also be seen that the width of the conducting band (above the Fermi energy level) for the SiNT is narrowed obviously, which means that the effective mass of carriers for the SiNT should be increased obviously as compared to that for Si bulk. Our calculation further suggests that the effective masses of carriers for SiB are $0.0025m_e$ at the top of valance band (VB), and $-0.0020m_e$ at the bottom of conducting band (CB), respectively. In comparison to bulk Si, however, a remarkably enhanced value of $0.034m_e$ near the Fermi energy level is obtained for the SiNT, which may be a main reason for its increased Seebeck coefficient. In addition, it can also be observed clearly that the electrons at the top of the VB (from -2 eV to 0 eV) in Si bulk mainly come from the p orbital and almost not from the s orbital, but the electrons at the bottom of CB (from 0 eV to $+2$ eV) are contributed both from the p orbital and the s orbital. Similarly, the electrons at the top of the VB for the SiNT are mainly from the p orbital while the electrons at the bottom of CB are contributed both from the p orbital and the s orbital. Consequently, two different bonding behaviors exist in bulk Si: the s orbital and the p orbital in sequence of the covalent bonding strength between the parent atoms, which would induce a discontinuous spectrum in the phonon DOS curve. In general, the electric conductivity is mainly determined by the DOS near the Fermi energy level.[34] The small DOS of 1.25 electrons/eV for the bulk Si may be a main reason for its low electrical conductivity. However, the DOS for the SiNT is increased to 40 electrons/eV, which is helpful for increasing its electrical conductivity. On the other hand, the Seebeck coefficient is determined by the effective mass and mobility of carriers.[35] Hence, an increased Seebeck coefficient for SiNTs can be expected for its large effective mass of carriers as compared to that for Si bulk. Pseudogap energy, an energy gap between the nearest two peaks near the Fermi energy level in the DOS curve, can reflect the covalent bonding strength between the parent atoms. It is clear that the pseudogap energy of bulk Si is 3.62 eV, which indicates a relatively strong covalent bonding and thus a higher phonon vibration frequency according to the formula $\omega = \sqrt{k/m}$ (ω is the phonon vibration frequency, k is the force constant, and m is the effective mass). However, the pseudogap of the SiNT is only 0.53 eV, meaning weakened covalent bonding, a lowered phonon vibration frequency, and thus a reduced phonon thermal conductivity.

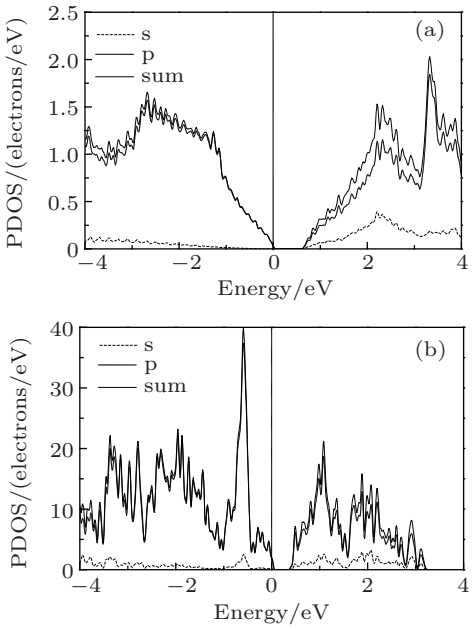


Fig. 1. DOS of bulk Si and the SiNT: (a) bulk Si; (b) SiNT.

3.2. Lattice dynamics

The phonon density of states for bulk Si and the SiNT is shown in Figs. 2(a) and 2(b), respectively. A gap at about 250 cm^{-1} can be observed in Fig. 2(a). Such a gap can be explained by the distribution of the bond lengths in the unit cell.[36] The existing two different covalent bonding behaviors (s orbital and p orbital) between Si atoms in the bulk Si show effectively two different force constants, which leads to the frequency gaps and the discontinuous spectrum in the phonon DOS curves. More importantly, the phonon DOS of the SiNT is decreased obviously as compared to that of bulk Si, which may be a main reason for its large reduction in phonon thermal conductivity.

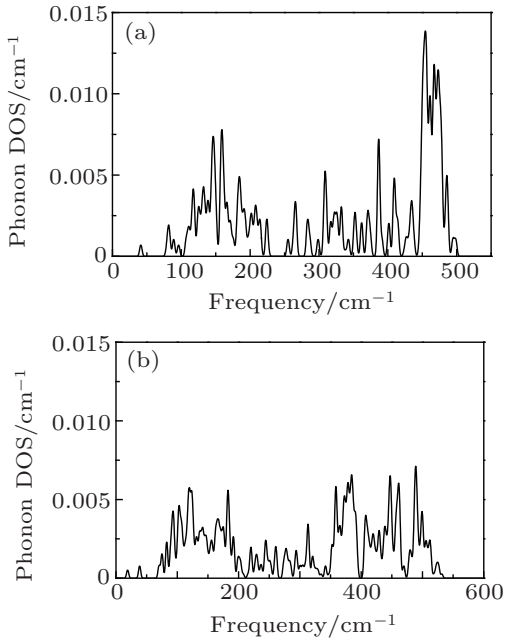


Fig. 2. Phonon DOS of bulk Si and the SiNT: (a) Si bulk; (b) SiNT.

The temperature dependence of the heat capacity and Debye temperature for bulk Si and the SiNT is shown in Fig. 3. The calculated heat capacity at room temperature is 10 cal/cell·K and 118 cal/cell·K for bulk Si and the SiNT, respectively. The total heat capacity includes two parts, one from the phonon contribution (C_p), and the other from the electron contribution (C_e). In a low temperature (below 300 K), the heat capacity coincides with the formula $C = AT^3$, which corresponds to C_p. At high temperature (above 300 K), however, the heat capacity is directly proportional to AT, which belongs to C_e. The calculated Debye temperatures for bulk Si and the SiNT at room temperature are 640 K and 605 K, respectively. Such a reduction in the Debye temperature for the SiNT will result in a decreased mean free path and thus a lowered phonon thermal conductivity. Figure 4 suggests the mean free path of phonons for bulk Si and the SiNT. It can be seen that the mean free path of the SiNT is smaller than that of the Si bulk, which is responsible for its large reduction in phonon thermal conduction.

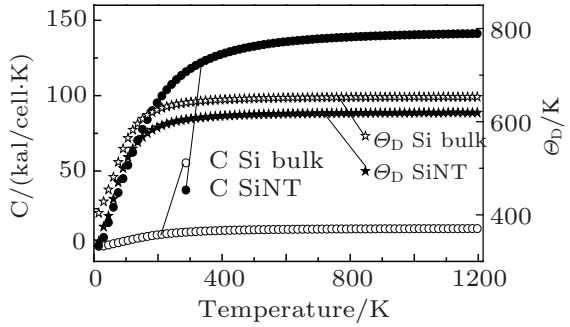


Fig. 3. Heat capacity and Debye temperature of the bulk Si and the SiNT.

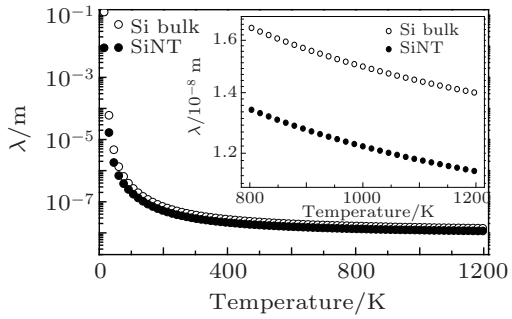


Fig. 4. Mean free path of the bulk Si and the SiNT.

3.3. Thermoelectric properties

The electrical conductivity and Seebeck coefficient for the bulk Si and the SiNT are presented in Fig. 5. It can be seen that the electrical conductivity of the bulk Si increases continuously with increasing temperature, indicating a typical semiconductor characteristic. However, the SiNT exhibits a typical semimetal behavior because of its negative temperature dependence of the electrical conductivity. In fact, the transition between semimetallic and semiconductor has been observed in Bi nanotubes.[13] The electrical conductivity at 1200 K for SiNT is increased by a factor of 3.5 from 129600 $\Omega^{-1}\cdot m^{-1}$ for bulk Si to 580000 $\Omega^{-1}\cdot m^{-1}$, which originates from its largely enhanced DOS near the Fermi energy level and a narrowed band gap. The negative sign of the Seebeck coefficients for the bulk Si and a SiNT indicates that the major carriers are electrons in the whole temperature. Moreover, the Seebeck coefficient of the SiNT at 1200 K is improved from 150 $\mu V\cdot K^{-1}$ for the bulk Si to 184 $\mu V\cdot K^{-1}$, which is well consistent with the experimental value of Si nanomaterials,[30] but is larger than that of the reported carbon nanotube.[37] Such an improvement in the Seebeck coefficient for the SiNT is attributed to its increased effective mass of carriers.[38]

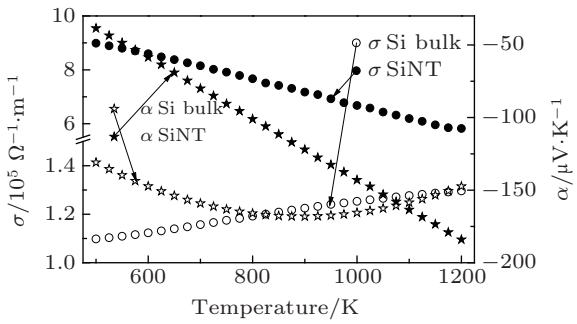


Fig. 5. Electrical conductivity and Seebeck coefficient of bulk Si and SiNT.

Figure 6 plots the total, electron, and phonon thermal conductivity of the bulk Si and the SiNT as functions of temperature. It is found that the total thermal conductivity κ of SiNT at 1200 K is reduced by 1 time from 43.8 $W\cdot m^{-1}\cdot K^{-1}$ for the bulk Si to 21.0 $W\cdot m^{-1}\cdot K^{-1}$. Such reduction in κ can also be observed in SiGe nanowires.[35] The κ is divided

into two parts: the electron thermal conductivity κ_e and the phonon thermal conductivity κ_p. It can be seen that the κ_e at 1200 K of SiNT is increased from 3.8 $W\cdot m^{-1}\cdot K^{-1}$ for bulk Si to 16.9 $W\cdot m^{-1}\cdot K^{-1}$ for its increased electrical conductivity. It should also be noted that the κ_p of SiNT at 1200 K is largely reduced by a factor of 8 from 40.8 $W\cdot m^{-1}\cdot K^{-1}$ for bulk Si to 4.5 $W\cdot m^{-1}\cdot K^{-1}$. This phenomenon can also be observed in other nanowires or nanotubes.[10,12,14]

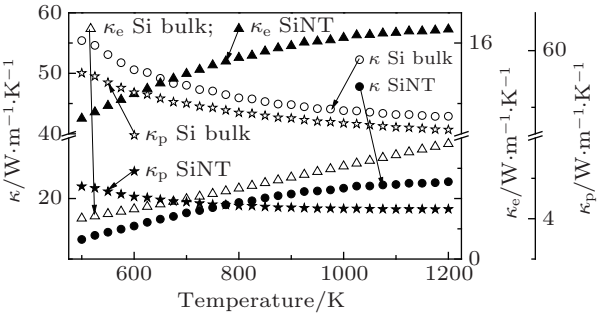


Fig. 6. Total, electron, and phonon thermal conductivity of the bulk Si and a SiNT.

Generally, the dominant mechanisms which have profound influences on thermal conductivity are: phonon–phonon scattering, charge-carrier–phonon scattering, and point-defect– phonon scattering. As for the bulk Si, the phonon–phonon scattering and the point defect scattering are the most important factors in reducing the thermal conductivity for short wavelength phonons at a low temperature, while the electron–phonon scattering is more effective for long-wavelength phonons at a higher temperature.[30] However, the phonon scattering will play an important role in the SiNT at both long and short wavelengths, which leads to a large reduction in thermal conductivity due to a decreased phonon DOS, a lowered phonon vibration frequency and a shortened mean free path of phonons.[39] Additionally, a negative temperature dependence of the κ_p for the SiNT is also observed clearly. It is well known that the κ_p is closely related to the mean free path of phonons. At a temperature above the Debye temperature, the average phonon amount is positively proportional to T in terms of the following formula:

$$n = \frac{1}{e^{\hbar\omega/k_B T} - 1} \approx \frac{k_B T}{\hbar\omega}, \tag{8}$$

where n is the average phonon amount, h is the reduced Plank constant, and ω is the phonon vibration frequency. As a result, the average phonon amount increases with increasing temperature, which would result in a more frequent collision of phonons and thereby a decreased mean free path of phonons. Thus, the observed negative temperature dependence of the κ_p is caused by an increased average phonon amount in a higher temperature.[25]

Figure 7 shows the figure of merit for the bulk Si and the SiNT. The ZT value at 1200 K of the SiNT can be enhanced by 12 times from 0.08 for the bulk Si to 1.10. The obtained ZT value for the SiNT is close to that of the Si nanowires with a cross section of 1 nm^2,[8] but is smaller than the value of the $^{28}Si^{29}_{1-x}Si_x$ nanowires.[9] We ascribe the large enhancement in ZT value for a SiNT to the largely increased electrical conductivity and the significantly suppressed phonon thermal conductivity even though its Seebeck coefficient is also slightly increased simultaneously.

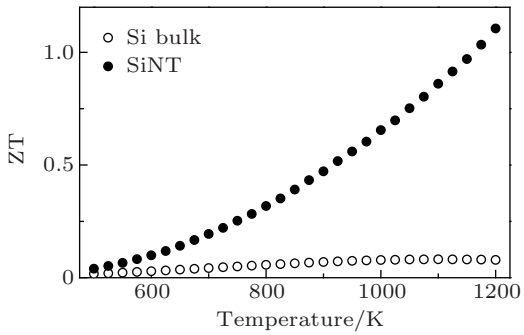


Fig. 7. Figure of merit of the bulk Si and the SiNT.

4. Conclusions

In conclusion, the electronic structures, the lattice dynamics, and the thermoelectric properties of the bulk Si and a SiNT have been calculated successfully using density functional theory and Boltzmann transport theory. The band gap for the bulk Si and the SiNT is 0.63 eV and 0.31 eV, respectively. The calculated DOS near the Fermi energy level for the bulk Si and the SiNT is 1.25 electrons/eV and 40 electrons/eV, respectively. The largely enhanced electrical conductivity of the SiNT originates from the increased DOS and the narrowed band gap. The improved Seebeck coefficient of the SiNT is attributed to the increased effective mass of carriers. The thermal conductivity of the SiNT is reduced by a factor of 1 as compared to that of the bulk Si, which results from the significant suppression of its phonon thermal conductivity caused by a weakened covalent bonding, a decreased phonon DOS, a lowered phonon vibration frequency, as well as a shortened mean free path of phonons.

References

[1] Yang M J, Shen Q and Zhang L M 2011 *Chin. Phys. B* **20** 106202
[2] Li H, Tang X F, Cao W Q and Zhang Q J 2009 *Chin. Phys. B* **18** 287
[3] Kim H, Kim I, Choi H J and Kim W 2010 *Appl. Phys. Lett.* **96** 233106
[4] Shi L H, Yao D L, Zhang G and Li B W 2010 *Appl. Phys. Lett.* **96** 173108
[5] Hochbaum A I, Chen R, Delgado R D, Liang W J, Garnett E C, Najarian M, Majumdar A and Yang P D 2008 *Nature* **451** 163
[6] Boukai A I, Bunimovich Y, Tahir-Kheli J, Yu J K, Goddard III W A and Heath J R 2008 *Nature* **451** 168
[7] Demchenko D O, Heinz P D and Lee B 2011 *Nanoscale Res. Lett.* **6** 502
[8] Liang G, Huang W, Koong C S, Wang J S and Lan J H 2010 *J. Appl. Phys.* **107** 014317
[9] Shi L H, Yao D L, Zhang G and Li B W 2009 *Appl. Phys. Lett.* **95** 063102

[10] Si H G, Wang Y X, Yan Y L and Zhang G B 2012 *J. Phys. Chem. C* **116** 3956
[11] Tan X J, Liu H J, Wen Y W, Lü H Y, Pan L, Shi J and Tang X F 2012 *Nanoscale Res. Lett.* **7** 116
[12] Tan X J, Liu H J, Wen Y W, Lü H Y, Pan L, Shi J and Tang X F 2011 *J. Phys. Chem. C* **115** 21996
[13] Zhou G, Li L and Li G H 2011 *J. Appl. Phys.* **109** 114311
[14] Chen J, Zhang G and Li B W 2010 *Nano Lett.* **10** 3978
[15] Pan L, Liu H J, Wen Y W, Tan X J, Lü H Y and Shi J 2010 *J. Comput. Theor. Nanosci.* **7** 1935
[16] Straumanis M E, Borgeaud P and James W J 1961 *J. Appl. Phys.* **32** 1382
[17] Segall M D, Lindan P J D, Probert M J, Pickard C J, Hasnip P J, Clark S J and Payne M C 2002 *J. Phys.: Condens. Matt.* **14** 2717
[18] Kohn W and Sham L J 1965 *Phys. Rev.* **140** A1133
[19] Marlo M and Milman V 2000 *Phys. Rev. B* **62** 2899
[20] Hammer B, Hansen L B and Norkov J K 1999 *Phys. Rev. B* **59** 7413
[21] Franscis G P and Payne M C 1990 *J. Phys: Condens. Matt.* **2** 4395
[22] Monkhorst H J and Pack J D 1977 *Phys. Rev. B* **16** 1946
[23] Li J C, Wang C L, Wang M X, Peng H, Zhang R Z, Zhao M L, Liu J, Zhang J L and Mei L M 2009 *J. Appl. Phys.* **105** 043503
[24] Murata M, Nakamura D, Hasegawa Y, Komine T, Taguchi T, Nakamura S, Jaworski C M, Jovovic V and Heremans J P 2009 *J. Appl. Phys.* **105** 113706
[25] Huang K 1979 *Solid State Physics* (Beijing: People's Education Press) p. 281 (in Chinese)
[26] Stiewe C, Bertini L, Toprak M, Christensen M, Platzek D, Williams S, Gatti C, Müller E, Iversen B B, Muhammed M and Rowe M 2005 *J. Appl. Phys.* **97** 044317
[27] Wang D, Tang L, Long M Q and Shuai Z G 2009 *J. Chem. Phys.* **131** 224704
[28] Kono Y, Ohya N, Taguchi T, Suekuni K, Takabatake T, Yamamoto S and Akai K 2010 *J. Appl. Phys.* **107** 123720
[29] Peng H, Wang C L, Li J C, Zhang R Z, Wang H C and Sun Y 2011 *Chin. Phys. B* **20** 046103
[30] Bux S K, Blair R G, Gogna P K, Lee H, Chen G, Dresselhaus M S, Kaner R B and Fleurial J P 2009 *Adv. Funct. Mater.* **19** 2445
[31] Ashcroft N W and Mermin N D 1976 *Solid State Physics* (New York: Harcourt Brace Press)
[32] Caillat T, Kulleck J, Borshchevsky A and Fleurial J P 1996 *J. Appl. Phys.* **79** 8419
[33] Goldsmid H J and Sharp J W 1999 *J. Electron. Mater.* **28** 869
[34] Ziman J M 1972 *Principles of the Theory of Solid* (Cambridge: Cambridge University Press)
[35] Cutler M, Leavy J F and Fitzpatrick R L 1964 *Phys. Rev.* **133** A1143
[36] Menon M, Richter E and Subbaswamy K R 1997 *Phys. Rev. B* **56** 12290
[37] Tsaousidou M and Papagelis K 2011 *Europhys. Lett.* **93** 47010
[38] Dresselhaus M S, Chen G, Ren Z, Fleurial J P, Gogna P, Tang M Y, Vashaee D, Lee H, Wang X, Joshi G, Zhu G, Wang D, Blair R, Bux S and Kaner R 2007 *MRS Proceedings* **1044** U02
[39] Henry A S and Chen G 2008 *J. Comput. Theor. Nanosci.* **5** 141